J Radioanal Nucl Chem (2014) 299:1635–1644
DOI 10.1007/s10967-013-2822-2

Radiosynthesis and biodistribution studies of [^{62}Zn/^{62}Cu]–plerixafor complex as a novel in vivo PET generator for chemokine receptor imaging

Ayuob Aghanejad · Amir R. Jalilian · Yousef Fazaeli · Davood Beiki · Behrooz Fateh · Ali Khalaj

Received: 18 September 2013 / Published online: 12 November 2013

Abstract In order to develop a possible C-X-C chemokine receptor type 4 (CXCR4) imaging agent for oncological scintigraphy, [^{62}Zn]labeled 1,1′-[1,4-phenylenebis(methylene)]bis-1,4,8,11-tetraazacyclotetradecane ([^{62}Zn]-AMD3100) was prepared using in-house made [^{62}Zn]$ZnCl_2$ and AMD-3100 for 1 h at 50 °C (radiochemical purity: >97 % ITLC, >96 % HPLC, specific activity: 20–22 GBq/mmol) in acetate buffer. The complex showed highly hydrophilic properties (log $P = -1.114$). Stability of the complex was checked in presence of human serum (37 °C) and in final formulation for 1 day. The biodistribution of the labeled compound in vital organs of wild-type Sprague–Dawdley rats were determined and compared with that of free Zn^{2+} cation up to 6 h. Co-incidence imaging of the complex was consistent with the distribution data up to 3 h. The complex can be a possible in vivo generator compound for PET imaging in CXCR4 positive tumors.

A. Aghanejad · D. Beiki
Research Center for Nuclear Medicine, Tehran University of Medical Sciences, Tehran, Iran

A. Aghanejad
Department of Radiopharmacy, Faculty of Pharmacy, Tehran University of Medical Sciences, Tehran, Iran

A. R. Jalilian (✉) · Y. Fazaeli
Nuclear Science and Technology Research Institute, Tehran 11365-3486, Iran
e-mail: ajalili@aeoi.org.ir

B. Fateh
Faculty of Engineering and Industrial Sciences (H38), Swinburne University of Technology, PO Box 218, Hawthorn, Victoria 3122, Australia

A. Khalaj
Department of Medicinal Chemistry, Faculty of Pharmacy, Tehran University of Medical Sciences, Tehran, Iran

Keywords ^{62}Zn · Production · AMD-3100 · Radiolabeling · Biodistribution · Co-incidence imaging

Introduction

The chemokine receptor subtype CXCR4 is an attractive target for cancer diagnosis and treatment as it is overexpressed on more than 70 % of human solid tumors, including mammary cancer, prostate cancer, B cell lymphoma, neuroblastoma, melanoma, cervical adenocarcinoma and glioma [1]. Moreover, it is involved in three fundamental aspects of cancer: primary tumor growth, cancer cell migration, and establishment of metastatic sites. Many peptidic and nonpeptidic ligands with different modes of antagonistic activity have been developed against this receptor [2].

Recent studies confirmed the necessity of CXCR4 in breast cancer metastasis [3] and imaging studies demonstrated that the CXCR4 is required to initiate proliferation and/or promote survival of breast cancer cells in vivo and suggest that CXCR4 inhibitors, such as; 1,1′-[1,4-phenylenebis(methylene)]bis-1,4,8,11-tetraazacyclotetradecane (AMD3100; Plerixafor), can improve treatment of patients with primary and metastatic breast cancers [4].

Previous studies have demonstrated that metals bound to the cyclam core increases the affinity of AMD3100 to the CXCR4 receptor, for instance, copper complex affinity is increased by 6-fold [5]. Also the binuclear $Zn^{(II)}$, $Cu^{(II)}$ and $Ni^{(II)}$ complexes of AMD3100 have shown to enhance the binding properties of AMD3100. Interestingly, the Zn(II)–AMD3100 complex (carrying overall +4 charge), revealed marginally higher specificity and reduced toxicity in vitro compared to the free ligand [6]. Also, it was

shown that the increased binding affinity of the single-metal ion substituted AMD3100 is obtained through enhanced interaction of one of the cyclam ring systems with the carboxylate group of CXCR4 receptor and not binuclear complexes [5].

To image CXCR4 expression in tumors using positron emission tomography (PET) and single photon emission tomography (SPECT) various groups have utilized the ability of the cyclam function of the prototype CXCR4 inhibitor AMD3100 to form strong complexes with radionuclides including Tc-99m [7], ^{64}Cu [8] has also shown the potentials in human xenograft imaging using PET [9].

^{62}Zn (HL = 6.9 h, EC: 3 %, β+: 97 %) is a rather long-half life PET radioisotope mostly used in preparation of ^{62}Zn/^{62}Cu generators, but its direct use has been rarely reported in labeling or imaging studies. [^{62}Zn] labeled bleomycin preparation had been reported as a possible PET imaging agent in tumor-bearing models [10] and in one study Zn–EDDA was reported as a pancreatic function agent [11].

To develop a possible imaging agent for CXCR4 expression in tumors we utilized the ability of the cyclam function of the prototype CXCR4 inhibitor AMD3100 to form a complex with ^{62}Zn to develop [^{62}Zn]-AMD3100 as a possible imaging agent for PET (Fig. 1).

Due to stability of copper–AMD3100 complex and physical transformation of ^{62}Zn to ^{62}Cu in the complex, a possible in vivo generator possessing PET imaging potential is pursued in this work.

Experimental

Production of ^{62}Zn was performed at the Nuclear Medicine Research Group (AMIRS) 30 MeV cyclotron (Cyclone-30, IBA). AMD3100 octa hydrochloride was purchased from the Sigma-Aldrich Chemical Co. (Germany); and the ion-exchange resins from Bio-Rad Laboratories (Canada). Thin layer chromatography (TLC) for cold compounds was performed on polymer-backed silica gel (F 1500/LS 254, 20 × 20 cm, TLC Ready Foil, Schleicher & Schuell®, Germany). Normal saline and sodium acetate used for labeling were of high purity and had been filtered through 0.22 μm Cativex filters. Instant thin layer chromatography (ITLC) was performed by counting Whatman No. 2 papers using a thin layer chromatography scanner, Bioscan AR2000, Bioscan Europe Ltd. (France). Analytical high performance liquid chromatography (HPLC) used to determine the specific activity, was performed by a Shimadzu LC-10AT, armed with two detector systems, flow scintillation analyzer (Packard-150 TR) and UV–visible (Shimadzu) using Whatman Partisphere C-18 column 250 × 4.6 mm, Whatman, NJ (USA). Analytical HPLC was also used to determine the specific radioactivity of the labeled compound. Biodistribution data were acquired by counting normal saline washed tissues after weighting on a Canberra™ high purity germanium (HPGe) detector (model GC1020-7500SL). Radionuclidic purity was checked with the same detector.

For activity measurement of the samples a CRC Capintec Radiometer (NJ, USA) was used. All calculations and ITLC counting were based on the 511 keV peak. Animal studies were performed in accordance with the United Kingdom Biological Council's Guidelines on the Use of Living Animals in Scientific Investigations, 2nd edn. For each time interval 3 rats were used. Images were taken in coincidence mode of a Dual-Head SPECT system (SMV, France, Sopha DST-XL).

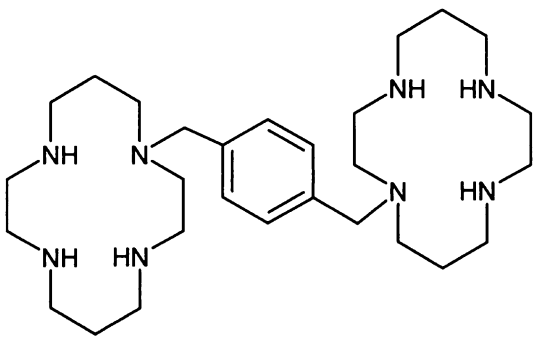

Fig. 1 Chemical structure of AMD3100

Targetry

A water-cooled copper target substrate was used for the irradiation. The beam hit at a slanting angle of 6°. The cooling was performed using a high flow-rate water stream. The target backside was equipped with the fine fins, to increase the cooling efficiency. The scheme of target is shown in Fig. 2. The thin layer of gold was electroplated on the Cu substrate to make a suitable under-coat medium. ^{62}Zn was obtained by ^{63}Cu(p,2n)^{62}Zn nuclear reaction using natural copper (69.2 % ^{63}Cu) as the target material. The optimum necessary thickness of electroplated Cu layer on the gold sub-layer was calculated by considering the excitation function data and energy degradation of protons in copper using SRIM code made on the bases of Ziegler's formulas [12]. Considering the 6° angle against the proton beam, the optimum target thicknesses of 118, 90, 74, 50, 36 and 23 μm were determined for 30, 27, 25, 22, 20 and 18 MeV proton respectively to reduce the energy below threshold (14 MeV) (Fig. 2).

All electroplating experiments were carried out in cylindrical plexy-glass cell with coaxial Pt-anode rod (dia. 1 mm), which had been made for electroplating of four target simultaneously. Au or Cu was electroplated on

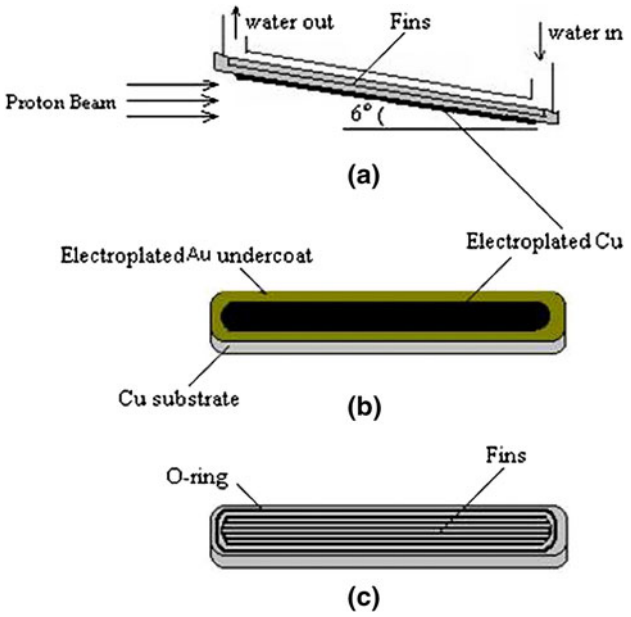

Fig. 2 A schematic drawing of the target; **a** target position during irradiation, **b** front side of the target with electroplated gold and Cu on the surface, **c** back side of the target with deep fins or canals for cooling water

surface area of 10 × 120 mm. A superimposed sinusoidal deposition waveform and high speed stirring rod (800 rpm) were applied for electroplating bath. This waveform is the sum of a sinusoidal alternating (ac) wave current or potential and a direct cathodic current (dc).

Gold electrodeposition

A gold containing bath was prepared according to reported method [13] with slight modifications. As the 6° glancing angle reduces the required target thickness by 10 fold, electroplating a 75-μm thick target was suitable. The target was irradiated by 22 MeV (150 μA) protons for 76 min.

Cu electroplating on gold sub-layer

Acidic copper solution containing copper sulfate and sulfuric acid were used for electroplating bath. In this experiment, the optimized concentration and operating conditions were determined: copper sulfate 200 g/l, sulfuric acid 80 g/l, temperature 25 °C and current density 3 A/dm^2. The thickness of electroplated Cu layer was determined by subtracting the target weight after and before electroplating.

Irradiation

The various energies of 18, 20, 22, 25, 27 and 30 MeV proton beams were used for the Cu target irradiation. For each target, the irradiation was carried out for 15 min at the current of 100 μA.

Chemical separation

All manipulations were carried out in a lead shield hot cell equipped with manipulator and semi-automated remotely controlled procedure. Target was fixed in plexy-glass target holder with pneumatic clapping system. Only the coated surface area had connection with solution, which transferred by means of a peristaltic pump to dissolve the Cu. The Cu layer was dissolved by 10–30 ml 8 N HNO_3(depending on the target thickness). While dissolving the copper, whenever the Ni sub-layer was appeared, the solution transfer was stopped. The radiochemical separation of the ^{62}Zn from the target was carried out with a method described with slight modifications [14, 15]. After dissolving the irradiated target, solution was heated under a flow of nitrogen to dry up until a precipitate was formed. The precipitate was rinsed two times by distilled water (10 ml) and a portion of 2 N HCl was added and mixed gently. The solution was pumped through a column 10 × 100 mm filled with Bio-Rad AG-1X8 resin and preconditioned with 2 N HCl. For the elution of ^{62}Zn in anion exchange resin, 0.005 N HCl was adopted instead of water used [16].

Quality control of the product

Control of radionuclide purity

Gamma spectroscopy of the final sample was carried out by counting in an HPGe detector coupled to a Canberra^{TM} multi-channel analyzer for 1,000 s.

Chemical purity control

This step was carried out to ensure that the amounts of zinc and copper ions resulting from the target material and backing in the final product are in the range of internationally accepted limits. Chemical purity was checked by differential-pulsed anodic stripping polarography. The detection limit of our system was 0.1 ppm for copper ions.

Preparation of [^{62}Zn]-AMD3100

The acidic solution (2 ml) of [^{62}Zn]$ZnCl_2$ (137 MBq, 3.7 mCi) was transferred to a 5 ml-borosilicate vial and heated to dryness using a flow of N_2 gas at 50–60 °C followed by the addition of acetate buffer (500 μl, pH 5). Fifty microlitres of AMD3100 octa hydrochloride dissolved in 0.1 M ammonium acetate pH 5 (1 mg/ml ≈ 1.26 micromol) was added to the zinc-containing vial and vortexed at 25, 50 and 80 °C separately. The active solution

was checked for radiochemical purity by ITLC and HPLC methods at 0.5, 1 and 2 h after labeling. The final solution of radiolabeled compounds was then passed through a 0.22 μm filter and pH was adjusted to 5.5–7.

Quality control of [^{62}Zn]-AMD3100

Radio thin layer chromatography

A 5 μl sample of the final fraction was spotted on the chromatography silica gel plates using 0.1 M sodium citrate solution as eluent and Whatman No. 2 paper and 10 % ammonium acetate:methanol (1:1) mixture as mobile phase.

High performance liquid chromatography

HPLC was performed with a flow rate of 1 ml/min, pressure: 130 kgF/cm^2 for 20 min. Radiolabeled compound was eluted using a mixture of two solutions (A: acetonitrile + 0.1 % TFA/water + 0.1 % TFA, 90:10) using reversed phase column Whatman Partisphere C_{18} 4.6 × 250 mm.

Determination of partition coefficient

Partition coefficient (log *P*) of [^{62}Zn]-AMD3100 was culated by the determination of *P* (*P* = the ratio of specific activities of the organic and aqueous phases). A mixture of 1 ml of 1-octanol and 1 ml of isotonic acetate-buffered saline (pH 7) containing approximately 3.7 MBq of the radiolabeled indium complex at 37 °C was vortexed 1 min and left 5 min. Following centrifugation at >1,200×*g* for 5 min, the octanol and aqueous phases were sampled and counted in an automatic well-type counter. A 500 μl sample of the octanol phase from this experiment was shaken again 2–3 times with fresh buffer samples. The reported log *P* values are the average of the second and third extractions from 3 to 4 independent measurements.

Stability tests

The stability of the complex was checked according to the conventional ITLC method [17]. A sample of [^{62}Zn]-AMD3100 (37 MBq) was kept at room temperature for 24 h while being checked by ITLC at time intervals in order to check stability in final product using above chromatography system. For serum stability studies, to 36.1 MBq (976 μCi) of [^{62}Zn]-AMD3100 was added 500 μl of freshly prepared human serum and the resulting mixture was incubated at 37 °C for 24 h, aliquots (5 μl) were analyzed by ITLC.

Biodistribution of [^{62}Zn]-AMD3100 in wild-type rats

To determine biodistribution, [^{62}Zn]-AMD3100 and $^{62}ZnCl_2$ solutions were administered to normal rats separately. A volume (50–100 μl) of final radioactive solution containing 6.6 MBq (180 μCi) radioactivity was injected intravenously to each rodent through their tail vein. The total amount of radioactivity injected into each rat was measured by counting the 1-ml syringe before and after injection in a dose calibrator with a fixed geometry. The animals were killed by CO_2 asphyxiation (after anesthesia induction using propofol/xylazine mixture) at selected times after injection at the exact time intervals and the specific activities of different organs were calculated. Dissection began by drawing blood from the aorta, followed by collecting various tissue samples. The samples were weighed and their specific activities were determined with an HPGe detector counting the area under the curve of the 511 keV peak. The tissue uptakes were calculated as the percent of area under the curve of the related photo peak per gram of tissue (ID/g%).

Imaging of [^{62}Zn]-AMD3100 in normal rats

0.1 ml volumes of the final [^{62}Zn]-AMD3100 solution containing 6.6 MBq activity were injected into the dorsal tail vein of healthy rats. The total amount of radioactive material injected into each rat was measured by counting the 1-ml syringe before and after injection in an activity meter with fixed geometry. The animals were relaxed by halothane and fixed in a suitable probe. Images were taken 5, 50, 120 and 180 min after administration of the radiopharmaceutical in coincidence mode. The useful field of view (UFOV) was 540 mm × 400 mm. The spatial resolution in the coincidence mode was 10 mm FWHM at the CFOV, and sensitivity was 20 Kcps/μCi/cc. Sixty four projections were acquired for 30 s per view with a 64 × 64 matrix. Each rat was studied for 3 h.

Results and discussion

Production

Targetry

The appearance of the targets after irradiation showed no hot and melted spots in coated area. In one case, the target was irradiated for 15 min by 150 μA proton beams and no hot spot or damage of coated material was reported.

Cu electroplating

The Cu^{2+} salts such as sulfate solutions are highly ionized. The addition of sulfuric acid to the sulfate solution is necessary for obtaining acceptable deposits. Change in sulfuric acid concentration had more influence than change in copper sulfate concentration on anode and cathode polarization and on solution conductivity.

Our experiments showed that adding a small amount of thio-urea as an additive can increase the hardening of electroplated Cu. In optimized bath conditions, the current efficiency was 98–99 %.

Irradiation and the yields

A comparison of the theoretical and experimental yields of ^{62}Zn via the ^{nat}Cu(p,xn) process is given in Fig. 3. The calculated yield value represents the maximum yield, which can be expected from a given nuclear process. Figure 4 demonstrates the determined cross sections from various works compared to ALICE code.

From a given excitation function, the expected yield of a product for a certain energy range (i.e. target thickness) can be calculated using the expression:

$$Y = \frac{N_L \cdot H}{M} I\left(1 - e^{-\lambda t}\right) \int_{E_1}^{E_2} \left(\frac{dE}{d(\rho \cdot x)}\right)^{-1} \sigma(E) dE,$$

where N_L is the Avogadro number, H the enrichment (or isotopic abundance) of the target nuclide, M the mass number of the target element, I the projectile current, ($dE/d(\rho \cdot x)$) the stopping power, $\sigma(E)$ the cross section at energy E, λ the decay constant of the product and t the time of irradiation.

The expected yield of ^{62}Zn was calculated from above formula applying the numerical methods for the integral calculation. $\sigma(E)$ was calculated by code [26] and ($dE/d(\rho \cdot x)$) derived from Ziegler formula [27].

The yield ratio of ^{63}Zn/^{62}Zn in different irradiation energies is given in Table 1.

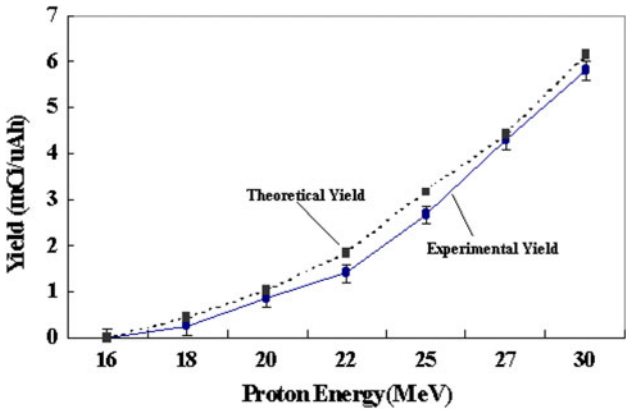

Fig. 4 Experimental and calculated yields of ^{62}Zn in function of the proton energy

Table 1 Yields of ^{63}Zn/^{62}Zn versus proton energy (end of bombardment)

Energy (MeV)	Yield of ^{63}Zn/^{62}Zn
18	>80
20	20.5
22	14.7
25	5.2
27	4.7
30	3.2

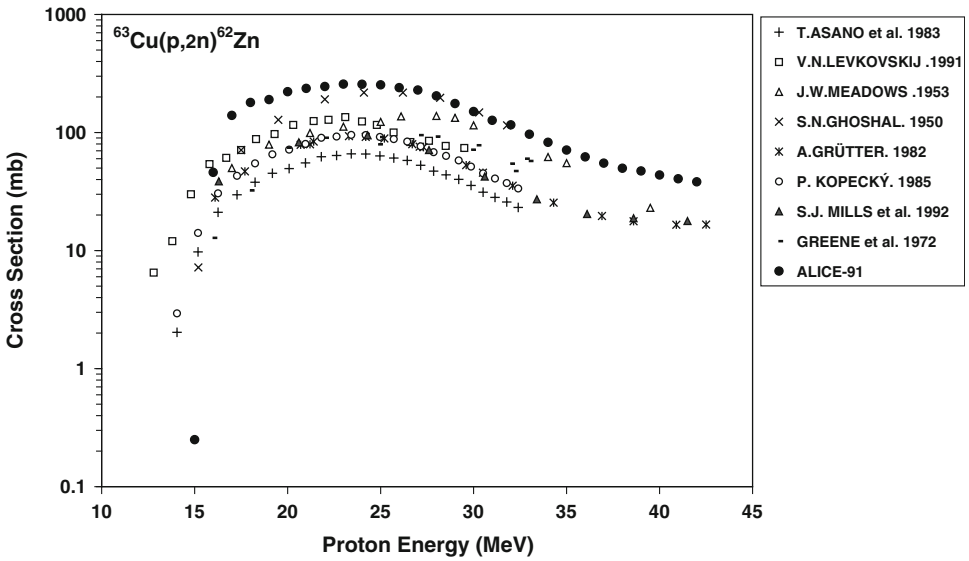

Fig. 3 Comparison of cross section calculations with the experimental data for ^{63}Cu(p,2n)^{62}Zn reaction [18–25]

Table 1 and Fig. 4 show that the higher proton energy enhances the production yield of ^{62}Zn relative to that of ^{63}Zn. Compared to the values reported by other scientists [28] the production yield of ^{62}Zn was higher in our condition (5.9 mCi/μAh vs 4.6 and 2.76 mCi/μAh reported by them, respectively) whereas the yield ratio of ^{63}Zn/^{62}Zn after irradiation was lower (3.2 vs 5.5 and 14.7, respectively). This is due to the higher energy of the protons (30 MeV vs 27 and 22 MeV, respectively) which favours the ^{63}Cu(p,2n) ^{62}Zn reaction relative to the ^{63}Cu(p,n) ^{63}Zn reaction.

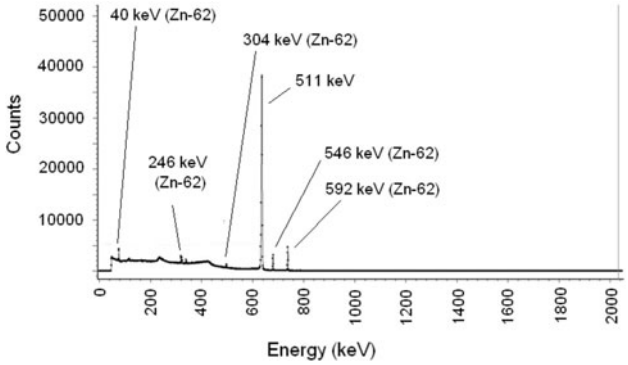

Fig. 6 Gamma spectrum of the final product in HPGe detector

Radiochemical separation

Radiochemical separation was performed by a two-step ion exchange chromatography method with a yield of higher than 95 %. Quality control of the product was performed in two steps. Figure 5 demonstrates the ^{62}Zn breakthrough activity of solution of the purified target resulting from the separation column.

Radionuclidic control showed the presence of gamma energies, all originating from ^{62}Zn and showed a radionuclidic purity higher than 99 % (E.O.S.). The presence of 40, 246, 304,546 and 592 keV photo-peaks was consistent with the reported gamma spectrum of ^{62}Zn radionuclide. However, the existence of 511 keV peak was also due to the presence of ^{62}Cu radionuclide as the decayed product of ^{62}Zn (Fig. 6). The concentration of copper (from target) was determined using polarography and shown to be below the internationally accepted levels, i.e. 0.1 ppm for Cu [29].

Using ammonium acetate 10 %:methanol (1:1) on Whatman No. 2 papers, the fast eluting species was observed at the R_f 0.9, related to ^{62}Zn cation, while any other Zn radiochemical species remained at the origin (not detected) (Fig. 7).

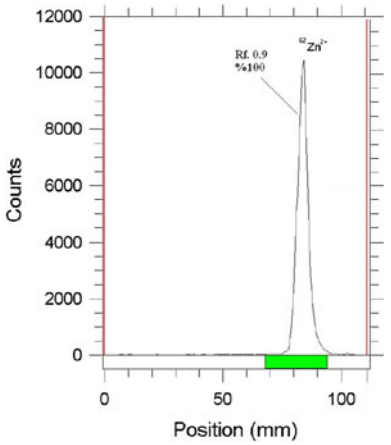

Fig. 7 ITLC of [^{62}Zn]$ZnCl_2$ in ammonium acetate 10 %:methanol (1:1) mixture on Whatman No. 2 papers

Radiolabeling

In the preparation of the most lipophilic complexes, organic solvent containing mixtures are usually used including, methanol:water, acetonitrile:water mixtures, however in this case none were able to distinguish $^{62}Zn^{2+}$

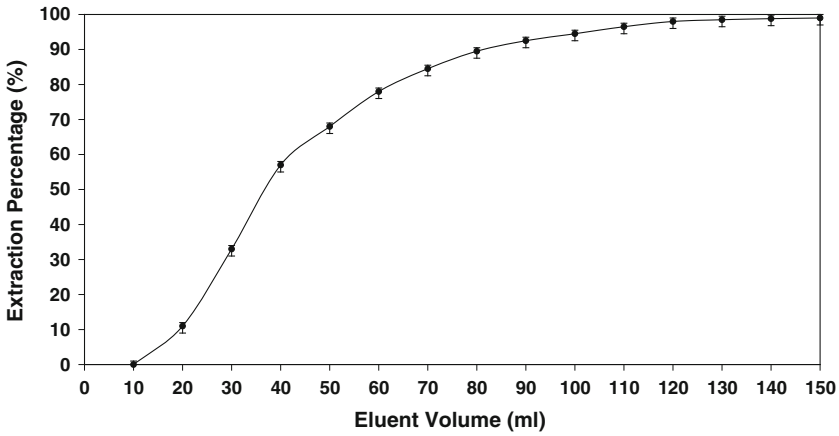

Fig. 5 Variation of zinc ion separation percentage with the eluent volume (0.05 N HCl) based on the ^{65}Zn tracer, $n = 5$, SE < 3 %

from the radiolabeled complex, that might be explained by the fact that the complex itself is a cationic species with significant polarity.

Thus various systems were used in this regard and two very polar systems on polar solid states worked well. This system was used also in the detection of the radiolabeled complex; a fast eluting species at R_f 0.9 was already shown to be Zn cation, while a slow eluted species was shown to be the radiolabeled compound at optimized conditions (Fig. 8).

It can be assumed that the nature of the radiolabeled complex is poly ionic as observed for Zn(II)AMD3100 complex with four cationic centers [6]. The cationic nature of the complex was also a major obstacle in HPLC radio analysis and a cationic column was preferable. However we used a reverse phase column in our settings and it worked with a tolerable difference in the retention times, enough for analytical measurements. The HPLC experiments using acetonitrile/water + 0.1 % TFA with a gradient protocol (10:90–90:10) was applied. In this system, free Zn eluted at 0.6 min while the complex was eluted at 1.52 min (scintillation detector) demonstrating a radiochemical purity of higher than 96 percent using optimized conditions without further purifications (Fig. 9).

At room temperature no detectable complex was formed. The best temperature was found to be 55–60 °C. At this temperature, when freshly prepared ^{62}Zn was used, all the radio-zinc was inserted into the complex, while heating the reaction mixture over 100 °C or for more than 1 h, the radiochemical yield dropped. The solution was stable at room temperature up to 24 h post-formulation, allowing performance of biological experiments. Before experiments, the solution passed through a 0.22 μm filter (Millipore).

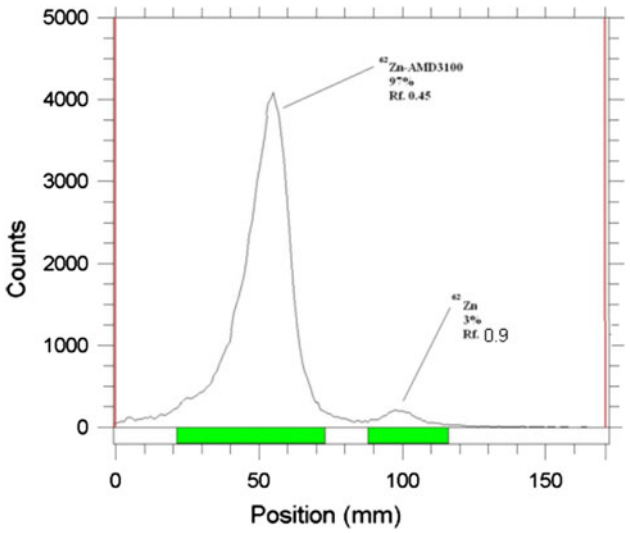

Fig. 8 ITLC of [^{62}Zn]-AMD3100 in ammonium acetate 10 %:methanol (1:1) mixture on Whatman No. 2 papers 1 h after labeling

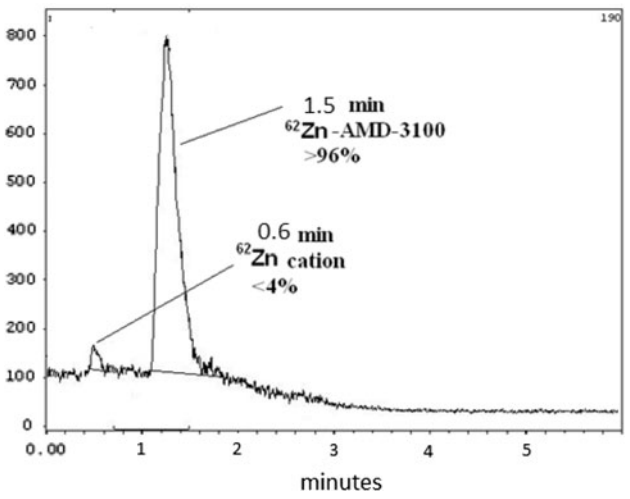

Fig. 9 HPLC chromatogram of [^{62}Zn]-AMD3100 solution on a reversed phase column using acetonitrile + 0.1 % TFA/water + 0.1 % TFA, gradient from 10:90 to 90:10

Partition coefficient of [^{62}Zn]-AMD3100

As expected, the lipophilicity of the [^{62}Zn]-AMD3100 compound is rather low. The measured octanol/water partition coefficient, P, for the complex was found to depend on the pH of the solution. At the pH 7 the log P was -1.114 ± 0.04. This is in agreement with the reported

Table 2 The stability of the radiolabeled complex in the presence of human serum at 37 °C and final formulation in 24 h using ammonium acetate 10 %:methanol (1:1) mixture on Whatman No. 2 papers

Stability (time):	4 h	8 h	12 h	24 h
Final preparation (%)	93 ± 1	92 ± 0.5	91 ± 0.8	90 ± 1
Human serum (%)	93 ± 1	90 ± 1	90 ± 2	88 ± 1

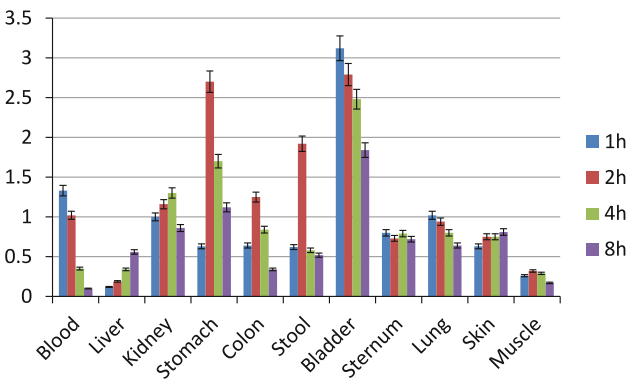

Fig. 10 Biodistribution of [^{62}Zn]$ZnCl_2$ (6.6 MBq, 180 μCi) in normal rats 1–8 h after iv injection via tail vein (ID/g%: percentage of injected dose per gram of tissue calculated based on the area under curve of 511 keV peak in gamma spectrum) ($n = 5$)

Zn–AMD3100 complex with four cationic centers which is also confirmed by late elution on Whatman ITLC.

Stability

Incubation of [^{62}Zn]-AMD3100 in freshly prepared human serum for 24 h at 37 °C showed no loss of ^{62}Zn from the complex. The radiochemical purity of complex remained at 90 % for 24 h under physiologic conditions. Table 2 demonstrates the stability data for the complex.

Biodistribution

For better comparison a biodistribution was performed for free Zn^{2+} as well. The ID/g% data are summarized in Fig. 10.

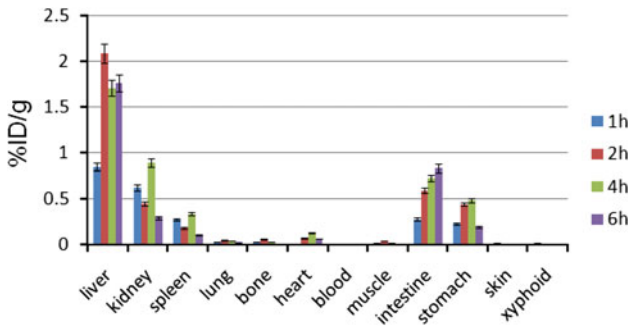

Fig. 11 Biodistribution of [^{62}Zn]-AMD3100 (1.85 MBq, 100 μCi) in wild rats 1–6 h after IV injection via tail vein (ID/g%: percentage of injected dose per gram of tissue calculated based on the area under curve of 511 keV peak in gamma spectrum) ($n = 5$)

The cation is mostly removed from the blood circulation within 8 h by excretion through the kidneys. The major activity content is rapidly transferred into bladder, which is agreement with other cations with 2+ charge. Another fraction of the cation is accumulated in liver. GI accumulation specially in stomach, colon and stool is also observed.

CXCR4 is abundantly expressed in normal tissues such as lungs, liver, and bone marrow and much less in other tissues [30]. Interestingly CXCR4 is absent in most of healthy tissue cell surfaces and as observed in Fig. 11, just the excretion tissues contain the activity. Unlike free cation, [^{62}Zn]-AMD3100 is not rapidly-washed-out through kidneys however urinary tract is still a major excretion route due to highly water soluble complex nature. As mentioned earlier liver cells are major receptor-rich cells in the body and a 30 % accumulation is observed in 3 h post injection.

The high stability of the complex predicted by in vitro methods does not allow the detachment of the radio cation into blood and other organs, thus kidneys are the most important excretion organs and also possible critical organ in the dosimetry calculations. Kidney, liver, spleen and lungs are only significant uptake targets. From the data it can be suggested that [^{62}Zn]-AMD3100 is metabolized and/or excreted through the kidneys and hepatic metabolism respectively. However no metabolic study performed to identify the natures of metabolite(s). The high kidney uptake can cause extra dose to surrounding critical tissues including gonads, this can be an obstacle, especially when using therapeutic radionuclides for therapy.

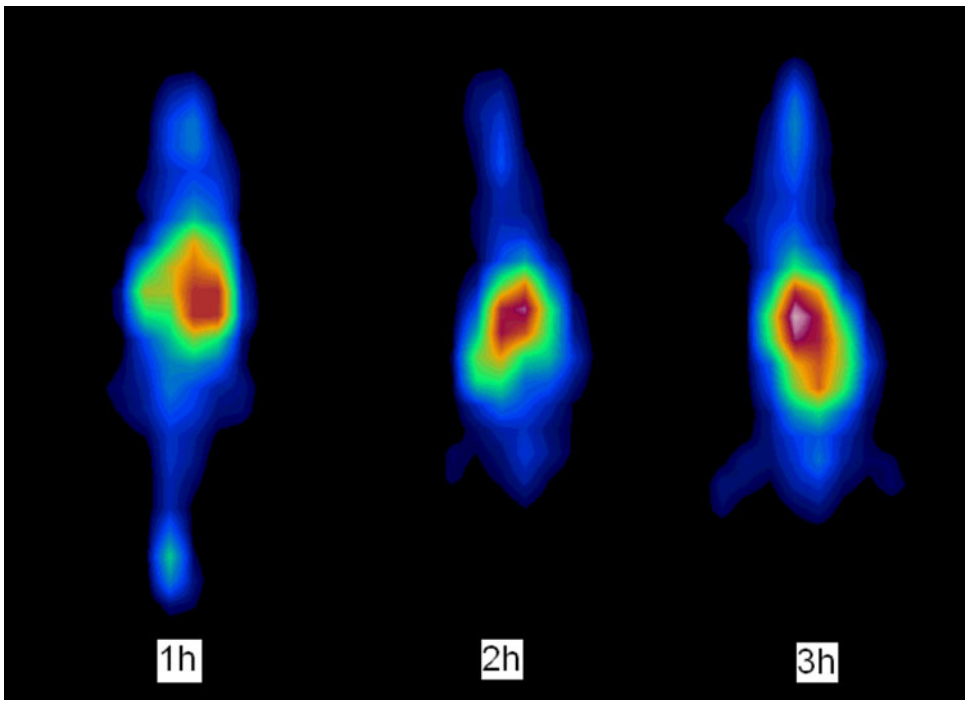

Fig. 12 Coincidence scans of [^{62}Zn]-AMD3100 (100 μCi), 1–3 h post injection

In a single report using ^{125}I-anti CXCR4 spleen has been shown to be a major site of accumulation, possibly due to the presence of CXCR4-containing blood cells. Also liver contain medial receptor sites at their cell surfaces [31]. With respect to this work, the major receptor rich organ (ID/g% = 2 at 2–4 h post injection), directly or indirectly can be considered the liver. However the high kidney uptake is a result of being the major excretion organ due to high water solubility of the complex, and not the receptor mediated uptake.

Co-incidence imaging of [^{62}Zn]-AMD3100 in wild type rats

The imaging was performed in the wild type rats up to 3 h post injection as shown if Fig. 12. The major activity accumulation in abdominal region in 1 h post injection is in agreement with distribution data obtained above consisting of liver, stomach and also kidneys. The pattern is almost constant in 3 h post injection.

Conclusion

[^{62}Zn]-AMD3100) was prepared using in-house made [^{62}Zn]$ZnCl_2$ and AMD-3100 for 1 h at 50 °C (radiochemical purity: >97 % ITLC, >96 % HPLC, specific activity: 20–22 GBq/mmol) in acetate buffer. The complex was stable in presence of human serum (37 °C) and in final formulation for 24 h. The biodistribution of the labeled compound in vital organs of wild-type Sprague–Dawdley rats demonstrated significant uptake in liver and spleen which have been shown to be major expression sites for CXCR4 in rats. [^{62}Zn]-AMD3100 is metabolized and/or excreted through the kidneys and also hepatic metabolism. Initial coincidence images and biodistribution results in wild type rats matched each other and demonstrate rapid wash out of the tracer from urinal tract. [^{62}Zn]-AMD3100 is suggested as a possible PET tracer for studies in CXCR4-positive tumor models.

Acknowledgments This study has been funded and supported by Tehran University of Medical Sciences, Tehran, Iran; Grant No. 18308. Authors wish to thank Ms. Moradkhani for performing animal tests and Ms. Bolourinovin for instrumental support.

References

1. Balkwill F (2004) Cancer and the chemokine network. Nat Rev Cancer 4:540–550
2. Masuda M, Nakashima H, Ueda T, Naba H, Ikoma R, Otaka A, Terakawa Y, Tamamura H, Ibuka T, Murakami T, Koyanagi Y, Waki M, Matsumoto A, Yamamoto N, Funakoshi S, Fujii N (1992) A novel anti-HIV synthetic peptide, T-22 ([Tyr5,12, Lys7]-polyphemusin II). Biochem Biophys Res Commun 189:845–850
3. Liang Z, Yoon Y, Votaw J, Goodman MM, Williams L, Shim H (2005) Silencing of CXCR4 blocks breast cancer metastasis. Cancer Res 65:967–971
4. Smith MC, Luker KE, Garbow JR, Prior JL, Jackson E, Piwnica-Worms D, Luker GD (2004) CXCR4 regulates growth of both primary and metastatic breast cancer. Cancer Res 64:8604–8612
5. Gerlach LO, Jakobsen JS, Jensen KP, Rosenkilde MR, Skerlj RT, Ryde U, Bridger GJ, Schwartz TW (2003) Metal ion enhanced binding of AMD3100 to Asp262 in the CXCR4 receptor. Biochemistry 42:710–717
6. Knight JC, Hallett AJ, Brancale A, Paisey SJ, Clarkson RWE, Edwards PG (2011) Evaluation of a fluorescent derivative of AMD3100 and its interaction with the CXCR4 chemokine receptor. Chem Bio Chem 12:2692–2698
7. Zhang JM, Tiana JH, Lia TR, Guo HY, Shen L (2010) ^{99m}Tc-AMD3100: a novel potential receptor-targeting radiopharmaceutical for tumor imaging. Chin Chem Lett 21:461–463
8. Jacobson D, Weiss ID, Szajek L, Farber J, Kiesewetter DO (2009) ^{64}Cu-AMD3100—a novel imaging agent for targeting chemokine receptor CXCR4. Bioorg Med Chem 17:1486–1493
9. Nimmagadda S, Pullambhatla M, Stone K, Green G, Bhujwalla ZM, Pomper MG, Morgan RH (2010) Molecular imaging of CXCR4 receptor expression in human cancer xenografts with [^{64}Cu]AMD3100-positron emission tomography. Cancer Res 70:3935–3944
10. Jalilian AR, Fateh B, Ghergherehchi M, Karimian A (2005) Development of [^{62}Zn]bleomycin as a possible PET tracer. Nukleonika 50:143–148
11. Fujibayashi Y, Saji H, Yomoda I, Kawai K, Horiuchi K, Adachi H, Torizuka K, Yokoyama A (1986) ^{62}Zn-EDDA: a radiopharmaceutical for pancreatic functional diagnosis. Int J Nucl Med Biol 12:439–446
12. Ziegler JF, Biersack JP, Littmark U (2000) The stopping and range of ions in matter. SRIM Code, Version 2000 XX
13. Weisberg AM (1990) Gold plating, 9th edn. ASM International, Metals Park, p 247
14. Green MA, Mathias CJ, Welch MJ, McGuire AH, Perry D, Fernandez-Rubio F, Perlmutter JS, Raichle ME, Bergmann RB (1990) Copper-62-labeled pyruvaldehyde bis(N_4-methylthiosemicarbazonato)copper(II): synthesis and evaluation as a positron emission tomography tracer for cerebral and myocardial perfusion. J Nucl Med 31:1989–1996
15. Bormans G, Janssen A, Adriaens P, Crombez D, Witsenboer A, DE Goeij J, Mortelmans L, Verbruggen A (1992) A ^{62}Zn/^{62}Cu generator for the routine production of ^{62}Cu-PTSM. Appl Radiat Isot 43:1437–1441
16. Green MA, Klippenstein DL, Tennison JR (1988) Copper(II) bis(thiosemicarbazone) complexes as potential tracers for evaluation of cerebral and myocardial blood flow with PET. J Nucl Med 29:1549–1557
17. Jalilian AR, Rowshanfarzad P, Sabet M, Novinrooz A, Raisali G (2005) Preparation of [^{66}Ga]bleomycin complex as a possible PET radiopharmaceutical. J Radioanal Nucl Chem 264:617–622
18. Asano T, Asano Y, Iguchi Y, Kudo H, Mori S, Noguchi M, Tahaka Y, Hirabayashi H, Ikeda H, Katoh K, Kondo K, Takasaki M, Tominaka T, Yamamoto A (1983) (p, xn),(p, pxn) and (p,2pxn) reactions medium-mass nuclei at 12 GeV. J Phys Rev Part C Nucl Phys 28:1840
19. Ghoshal SN (1950) An experimental verification of the theory of compound nucleus. J Phys Rev 80:939
20. Greene MW, Lebowitz E (1972) Proton reactions with copper for auxiliary cyclotron beam monitoring. Int J Appl Radiat Isot 23:342–344

21. Grütter A (1982) Excitation functions for radioactive isotopes produced by proton bombardment of Cu and Al in the energy range of 16 to 70 MeV. J Nucl Phys Sect A 383:98–108
22. Kopecký P (1985) Proton beam monitoring via the Cu(p, x)58Co, 63Cu(p,2n)62Zn and 65Cu(p, n)65Zn reactions in copper. Int J Appl Radiat Isot 36:657–661
23. Levkovskij VN (1991) Activation cross section nuclides of average masses (A = 40–100) by protons and alpha-particles with average energies (E = 10–50 Mev) by protons and alphas, Moscow. Data downloaded via the internet from the IAEA nuclear data section (experimental nuclear reaction data, http://www.nndc.bnl.gov/Exfor)
24. Meadows JW (1953) Excitation functions for proton-induced reactions with copper. J Phys Rev 91:885–887
25. Mills SJ, Steyn GF, Nortier FM (1992) Experimental and theoretical excitation functions of radionuclides produced in proton bombardment of copper up to 200 MeV. Int J Appl Radiat Isot 43:1019–1030
26. Blann M (1975) University of Rochester Report C00-3494-29
27. Ziegler JF, Biersack JP, Littmark U (1985) The stopping and range of ions in solids, vol 1 of the stopping and ranges of ions in matter. Pergamon Press, Elmsford
28. Robinson GD Jr, Zielinski FW, Lee AW (1980) The Zn-62/Copper-62 generator: a convenient source of copper-62 for radiopharmaceuticals. Int J Appl Radiat Isot 31:111–116
29. United States Pharmacopoeia 28, 2005, NF 23, p 1009
30. Woodard LE, Nimmagadda S (2011) CXCR4-based imaging agents. J Nucl Med 52:1665–1669
31. Nimmagadda S, Pullambhatla M, Pomper MG (2009) Immunoimaging of CXCR4 expression in brain tumor xenografts using SPECT/CT. J Nucl Med 50:1124–1130